Applied Thermal Engineering 29 (2009) 1657–1675

Contents lists available at ScienceDirect

Applied Thermal Engineering

journal homepage: www.elsevier.com/locate/apthermeng

A new engine indicating measurement procedure for combustion heat release analysis

Andre Valente Bueno [a], José Antonio Velásquez [b,c,*], Luiz Fernando Milanez [d]

[a] Mechanical Engineering Department, Federal University of Ceara, Brazil
[b] Mechanical Engineering Department, Pontifical Catholic University of Parana, Brazil
[c] Mechanical Engineering Department, Federal Technical University of Parana, Brazil
[d] Faculty of Mechanical Engineering, University of Campinas, Brazil

ARTICLE INFO

Article history:
Received 22 February 2007
Accepted 15 July 2008
Available online 5 August 2008

Keywords:
Engine indicating measurement
Engine combustion diagnosis
Combustion heat release analysis

ABSTRACT

This paper presents a new arrangement for the indicating measurement system utilized in the study of internal combustion engines. In this experimental configuration, the current polarized by a piezoelectric pressure transducer is converted into an analog signal proportional to the cylinder pressure variation rate, which constitutes the primary information for combustion heat release analysis. The proposed technique reduces the uncertainty in the pressure derivative data, providing more accurate heat release results than those obtained with the traditional transducer signal conditioning procedure, which requires the numerical derivation of in-cylinder pressure data supplied by a charge amplifier.

1. Introduction

In-cylinder pressure measurements are fundamental for engine combustion diagnosis and for indicated work calculation. In engine combustion diagnosis, the apparent heat release rate and the combustion reaction extent are the most useful quantities obtainable from in-cylinder pressure data. The apparent heat release rate is calculated by computing the amount of fuel chemical energy release necessary to obtain the pressure variations observed experimentally, while the combustion reaction extent is evaluated through the released fraction of the total fuel chemical energy [1–4].

Heat release analysis is often complemented using optical techniques [5–10] and its utilization as a diagnostic tool covers a wide range of objectives, including the development of new combustion systems, the analysis of alternative fuel burning, the validation of mathematical models for engine simulation, the investigation of combustion chamber insulation effects and the study of new injection strategies.

It is widely recognized that the reliability of heat release results strongly depends on the accuracy of the engine indicating measurements and especially on the accuracy of the cylinder pressure derivative [2–4]. Traditionally, the pressure derivative has been evaluated by numerical derivation of pressure data measured with a piezoelectric transducer polarized by a charge amplifier, a procedure that enhances the uncertainties present in pressure data and imposes spurious oscillations to the heat release results.

Taking into account the relevance of the accurate determination of the pressure derivative to improve the heat release results, an engine indicating procedure that allows the direct measurement of the pressure variation rate is proposed in this work. Experiments conducted with a direct-injection, turbocharged, high-speed diesel engine show that the proposed procedure allowed a reduction in the uncertainty of the pressure derivative data and in the noise level of the calculated heat release results, as compared with those obtained from measurements carried out using the traditional procedure.

2. Experimental apparatus

A ZÖLLNER ALPHA-160 dynamometer and an AVL Puma 5 automated test bed system were employed to control engine operation and to evaluate its relevant performance characteristics. The tested engine was a direct-injection, turbocharged, high-speed diesel MWM 6.07T GMT-400, with the specification shown in Table 1. The engine intake was connected to a surge tank and the intake air flow rate was determined through the use of a rotary piston gas meter. Additionally, fuel consumption was measured using an AVL 733-S gravimetric fuel balance and water fed heat exchangers were used to control the engine coolant and fuel temperatures.

A schematic representation of the engine indicating system is provided in Fig. 1, and shows how this system was prepared to operate with the two measurement procedures addressed in the present work. An AVL 3066 charge amplifier was employed for the transducer polarization during the measurement of in-cylinder

* Corresponding author. Address: Mechanical Engineering Department, Pontifical Catholic University of Parana – PUCPR, Rua Imaculada Conceicao, 1155, 80215-901 Curitiba, PR, Brazil. Tel.: +55 41 3271 1323; fax: +55 41 3271 1349.
E-mail address: jose.velasquez@pucpr.br (J.A. Velásquez).

1359-4311/$ - see front matter © 2008 Elsevier Ltd. All rights reserved.
doi:10.1016/j.applthermaleng.2008.07.023

Table 1
Engine specification

Configuration	Four stroke, direct-injection
Turbocharger control	Waste gate valve
Number of cylinders	6
Displacement (dm^3)	4.2
Bore (m)	0.093
Stroke (m)	0.103
Rod length (m)	0.170
Compression ratio	17.8:1
Valves per cylinder (intake/exhaust)	2/1
Intake valves close (°after BDC)	32
Exhaust valve opens (°before BDC)	55
Fuel injection pump	Bosch VE
Fuel injectors	Five holes
Fuel injectors opening pressure (first/second stage) (bar)	220/300
Maximum power (kW)	123
Maximum power speed (rpm)	3400

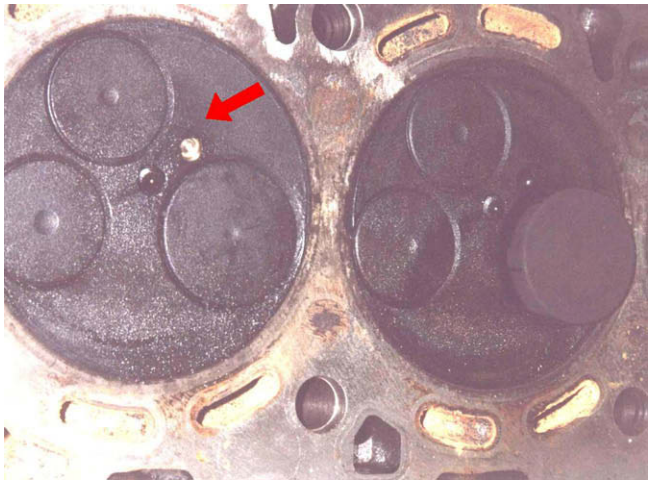

Fig. 2. Installation position of the pressure transducer.

pressure, while a current-to-voltage converter was utilized during the measurement of the cylinder pressure derivative. The circuitry used in the construction of a current-to-voltage converter that is appropriate for engine indicating measurements is presented in Section 3.2. A piezoelectric miniature pressure transducer AVL GM 12 D was used for cylinder pressure measurement as well as for pressure derivative measurement. This transducer was flush mounted above the piston bowl (see Fig. 2), thus preventing pressure oscillations inherent to the squish gap and to mounting channels [11]. The angular position of the top dead center was determined dynamically, using an AVL 428 TDC capacitive sensor.

The pressure and the pressure derivative signals were sampled at a 0.5° c.a. resolution and were averaged over 56 consecutive cycles, using an AVL Indimeter 617 indicating data acquisition system with 12 bit resolution. The measuring chain formed of the piezoelectric transducer, the charge amplifier and the data acquisition system was calibrated prior to measurements, following the quasistatic procedure described by Lancaster et al. [12] and using a Web Meβgerätewerk dead-weight tester with INMETRO traceability. Further details regarding calibration of the proposed arrangement of the indicating system are provided in Section 3.2.

In order to compare the proposed and the traditional engine indicating procedures, the same conditions of coolant temperature, fuel temperature, air flow rate, intake and exhaust manifold temperatures and pressures, engine speed and engine brake torque were used. Accordingly, heat release calculations from experimental data provided by both procedures were performed using the same values of cylinder wall temperatures and adjusting coefficients of the heat transfer correlation.

3. Signal conditioners for the piezoelectric pressure transducer

Engine indicating measurements for combustion diagnosis requires a durable transducer with high linearity, adequate frequency response and high resistance to thermal load, therefore, in-cylinder pressure measurements are usually carried out by

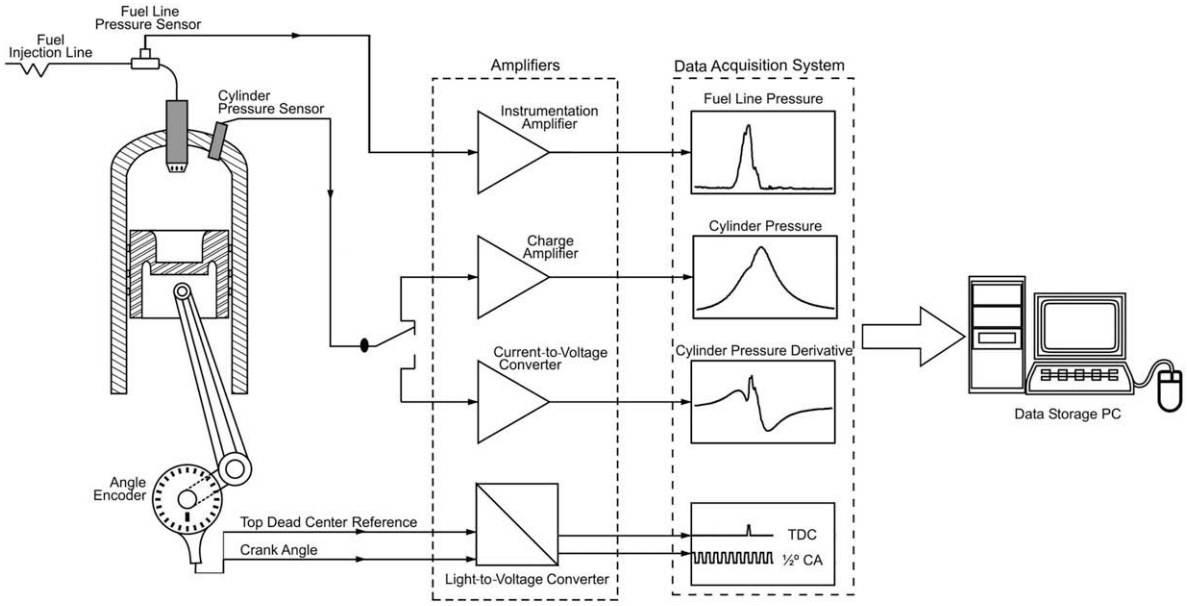

Fig. 1. System for measuring in-cylinder pressure and pressure derivative.

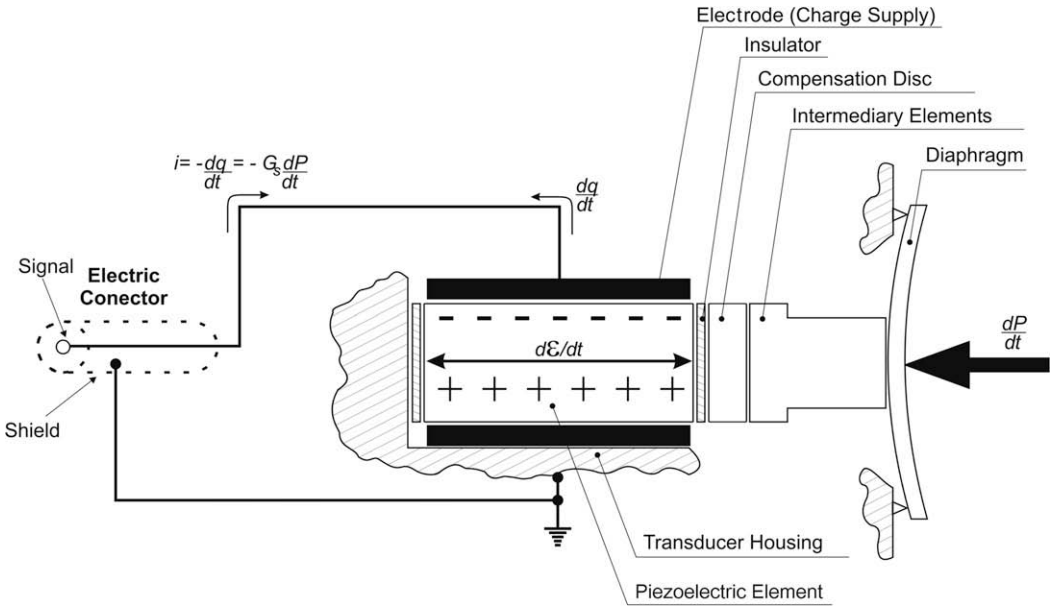

Fig. 3. The piezoelectric pressure transducer.

means of piezoelectric crystal transducers. Fig. 3 illustrates the principle of operation of such a pressure sensor. The pressure variation rate (dP/dt) experienced by the transducer diaphragm is transmitted to a piezoelectric crystal through intermediate elements, causing its deformation at a rate of $d\varepsilon/dt$. Due to the piezoelectric effect, this deformation polarizes charge q in the transducer electrode originating an electric current i, which constitutes the transducer output signal:

$$i = -\frac{dq}{dt} = -G_s \frac{dP}{dt} \quad (1)$$

where G_s is the transducer sensitivity.

Piezoelectric transducers only respond to pressure variations and, for this reason, the evaluation of actual in-cylinder pressure necessitates the determination of an appropriate pressure data baseline for each engine cycle. In this study, the data baseline was determined by choosing a pressure value at the intake valves closing that guarantees zero heat release rate during the first 80° c.a. of the compression stroke. This procedure follows the recommendations of Lapuerta et al. [13], who demonstrated that the pressure reference level is the only input parameter that significantly affects the heat release results during the initial phase of compression.

The accuracy of a piezoelectric pressure transducer deteriorates when it is exposed to a variable heat flux, as occurs during the combustion process [14]. As the sensor temperature varies, thermal strain arise in the sensor diaphragm and shell, changing the sensitivity of the piezoelectric element and producing a distortion in the transducer output signal, which is known as temperature drift [15]. Therefore, it can be seen that reducing the effects of temperature drift on the output signal is an important issue for the improvement of engine indicating techniques.

It is usual to divide temperature drift into a short-term and long-term component. Short-term drift, known as thermal shock, results from the heat flux variations within each cycle and causes pressure readings to be slightly higher than the actual cylinder pressure during combustion and slightly smaller during the remaining part of the power stroke. It cannot be readily identified or suppressed during signal processing, and may endanger the reliability of cylinder pressure data [11,14–20]. In this study, the extension of the short-term drift was assessed using the test procedure proposed by Randalph [19,20], and it was found to be compatible with data reported for transducers similar to that employed here [20].

The second component of the temperature drift, the so-called long-term drift or load-change drift, results from gradual variation of the transducer temperature due to changes in the engine operating conditions. As will be seen in the following sections, long-term drift affects in different ways the pressure data obtained from

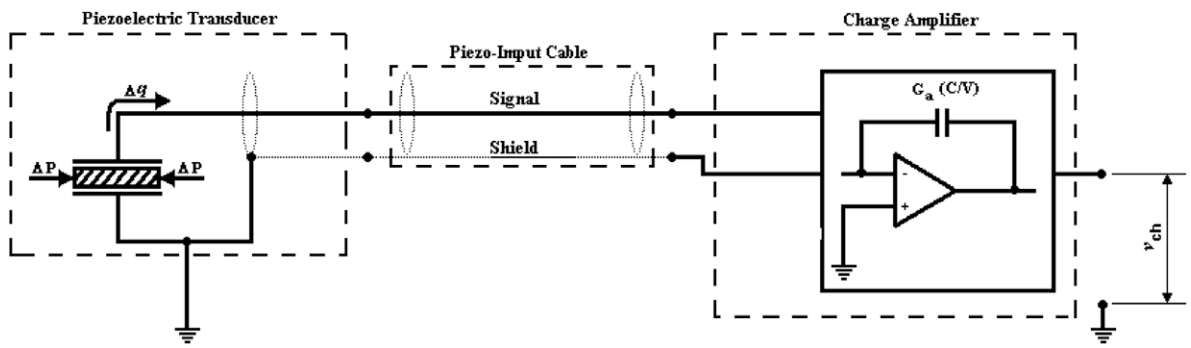

Fig. 4. Transducer signal conditioning through a charge amplifier.

each of the transducer signal conditioning procedures considered in this study.

3.1. The conventional technique for transducer signal conditioning

Fig. 4 shows a simplified scheme of the experimental assembly normally utilized for engine indicating measurements, which is based on an integral method of transducer signal conditioning. A high insulation shielded cable conducts the charge polarized by the transducer toward the charge (piezoelectric) amplifier. This equipment produces an output signal proportional to the time integral of the input current. Thus, the in-cylinder pressure P is related to the output voltage of the charge amplifier v_{ch} through the following expression:

$$(P - P_{ref}) = \frac{v_{ch} \cdot G_a}{G_s} \tag{2}$$

where P_{ref} is the in-cylinder pressure at the beginning of the integration operation and G_a is the gain of the charge amplifier.

The charge produced by the piezoelectric pressure transducer is very weak, reaching only a few dozens of pC/bar, so that leakage current in the measuring system has a significant impact on the integrated signal, causing a slow and continuous decrease in the output voltage, and resulting in underestimated pressure values. In order to reduce this negative effect to a tolerable level it is necessary to use a high impedance charge amplifier, as well as to maintain the electrical connections of the measuring system spotlessly clean. This instrumentation non-ideality combined with the integration of the long-term drift error (load-change drift) causes instability in the pressure data baseline. In literature, this instability is known as pressure data baseline drift or shift [11,17,18,21] and due to its effect the baseline may be rapidly displaced by several bars. Therefore, in-cylinder pressure measurement requires the periodic reset of the charge amplifier to avoid saturation.

When this technique for transducer signal conditioning is employed it is usual to obtain the pressure derivative through numerical manipulation of pressure data. In this study, this was accomplished using the following expression, which is based on fourth order finite differences [22]:

$$\frac{dP}{d\theta_j} = \frac{P_{j-2} - 8P_{j-1} + 8P_{j+1} - P_{j+2}}{12\Delta\theta} \tag{3}$$

where $\Delta\theta$ is the crank angle step between two consecutive pressure readings (0.5° c.a.). In an attempt to avoid the numerical derivation of the pressure data, Marzouk and Watson [18] tested the electronic derivation of the pressure signal provided by a charge amplifier. These authors did not obtain satisfactory results for the pressure variation rate, underestimating its peak value during premixed

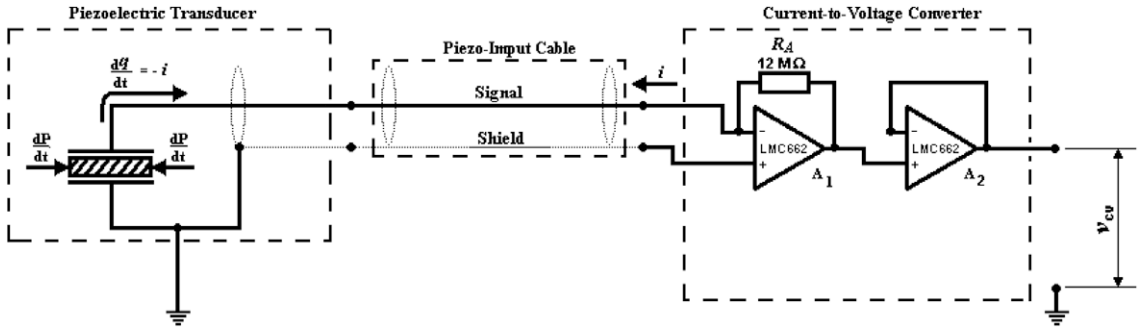

Fig. 5. Transducer signal conditioning through a current-to-voltage converter.

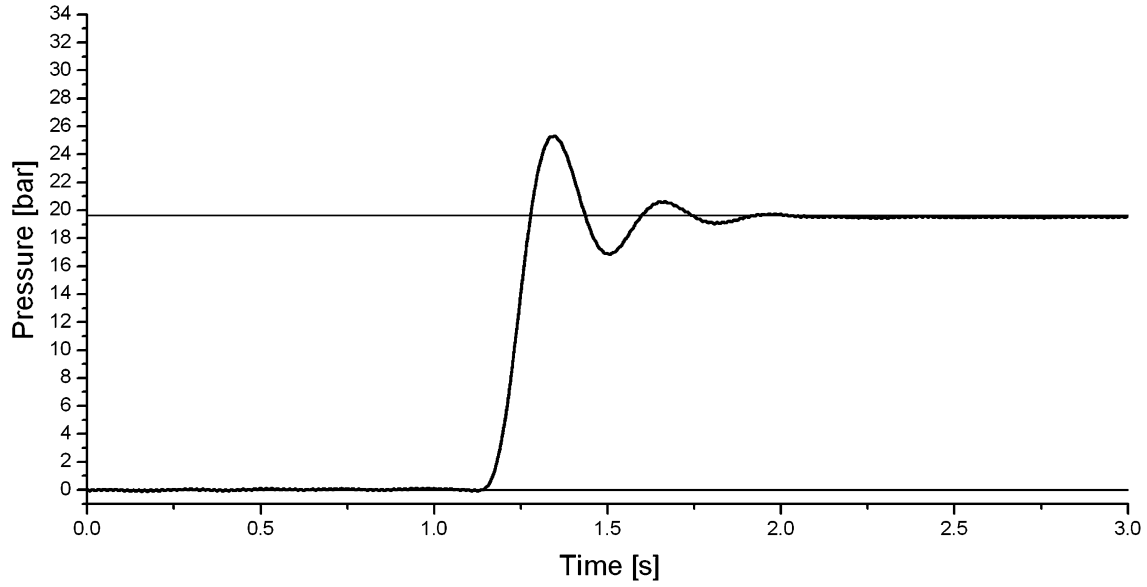

Fig. 6. Calibration pressure signal for the current-to-voltage converter.

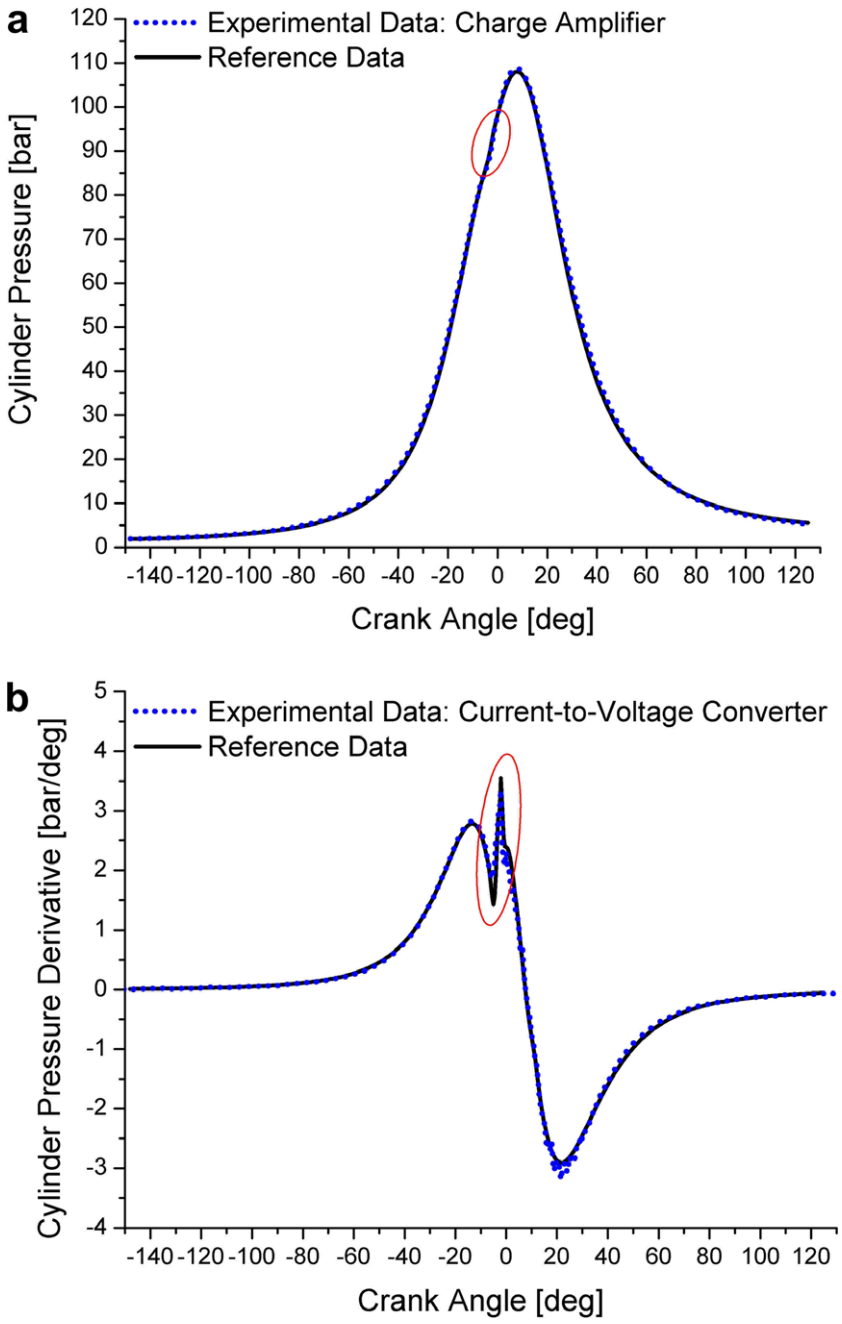

Fig. 7. Reference curves for pressure and pressure derivative data (2600 rpm and 80% of full load).

combustion. This was due to the inadequate frequency response of the analogical differentiation circuit, which severely affected its performance when processing the high frequency spectral components of the pressure signal.

3.2. The proposed procedure for transducer signal conditioning

Measuring in-cylinder pressure derivative demands the conversion of the current supplied by a piezoelectric pressure transducer into a voltage signal. The frequency response requirements in engine indicating measurements make it necessary to perform this conversion in a low input impedance device. Otherwise, an equivalent RC circuit formed by the transducer self-capacitance and by the input impedance of the signal conditioner may lead to attenuation and phase shift of the pressure derivative signal. As shown by Payri et al. [23], the shape of the combustion heat release rate is very sensitive to phase angle errors in the indicating data.

The current-to-voltage converter circuit shown in Fig. 5 attends the gain and the frequency response requirements for engine indicating measurements. This equipment has low input impedance, as given by the ratio of the gain adjustment resistance R_A to the open loop gain of the operational amplifier A_1, thus avoiding the influence of the piezoelectric transducer self-capacitance. The measured pressure variation rate is given by

$$\frac{dP}{dt} = \frac{v_{cv}}{G_s \cdot R_A} \tag{4}$$

where v_{cv} is the output signal of the current-to-voltage converter.

When this procedure for transducer signal conditioning is used, the pressure data may be obtained through numerical integration. In this study, a fourth-order Runge–Kutta method was used.

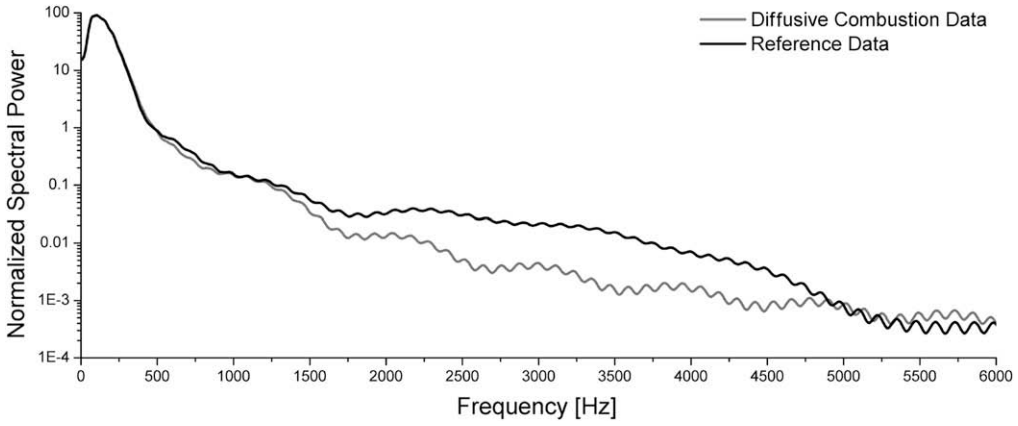

Fig. 8. Spectral distribution for simulated in-cylinder pressure derivative (2600 rpm and 80% of full load).

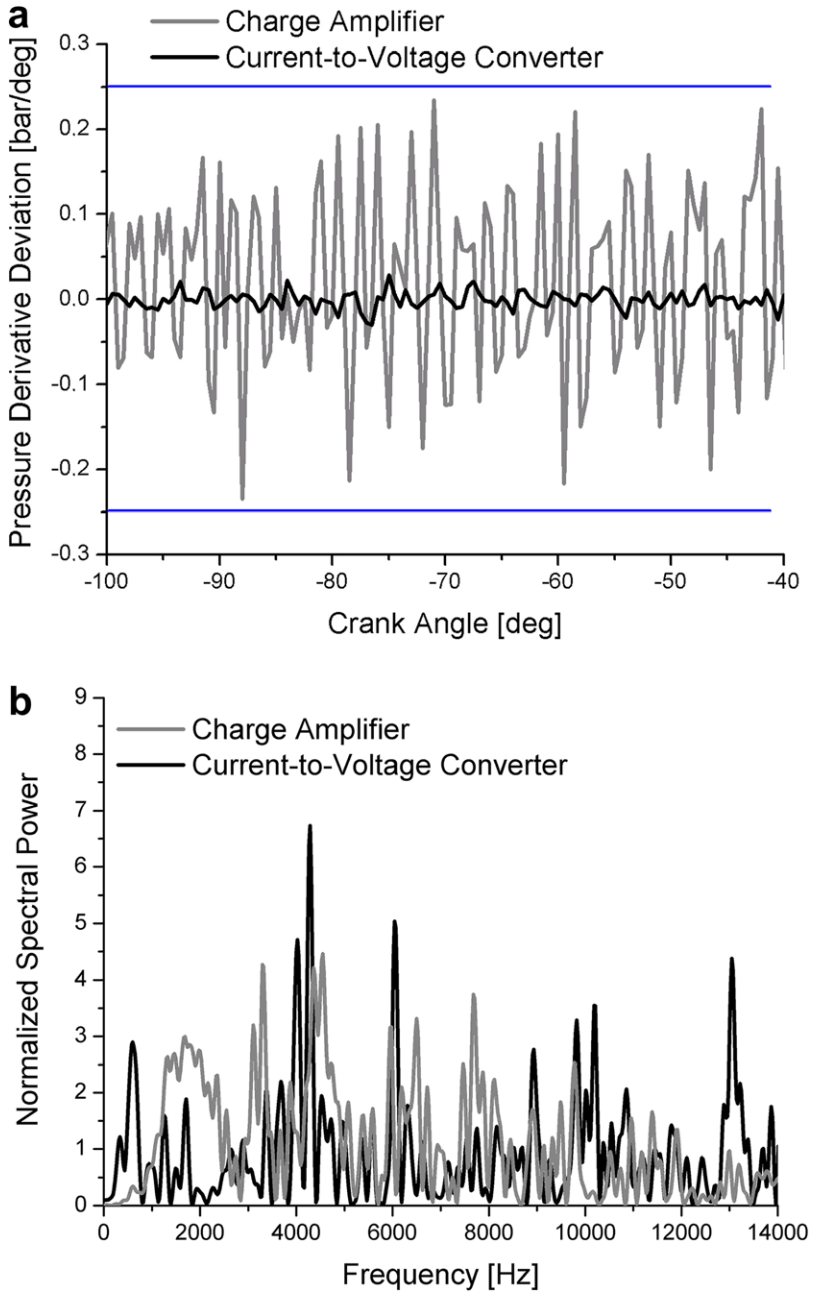

Fig. 9. Deviations due to the measurement system noise and to the in-cylinder flow (2600 rpm and 80% of full load).

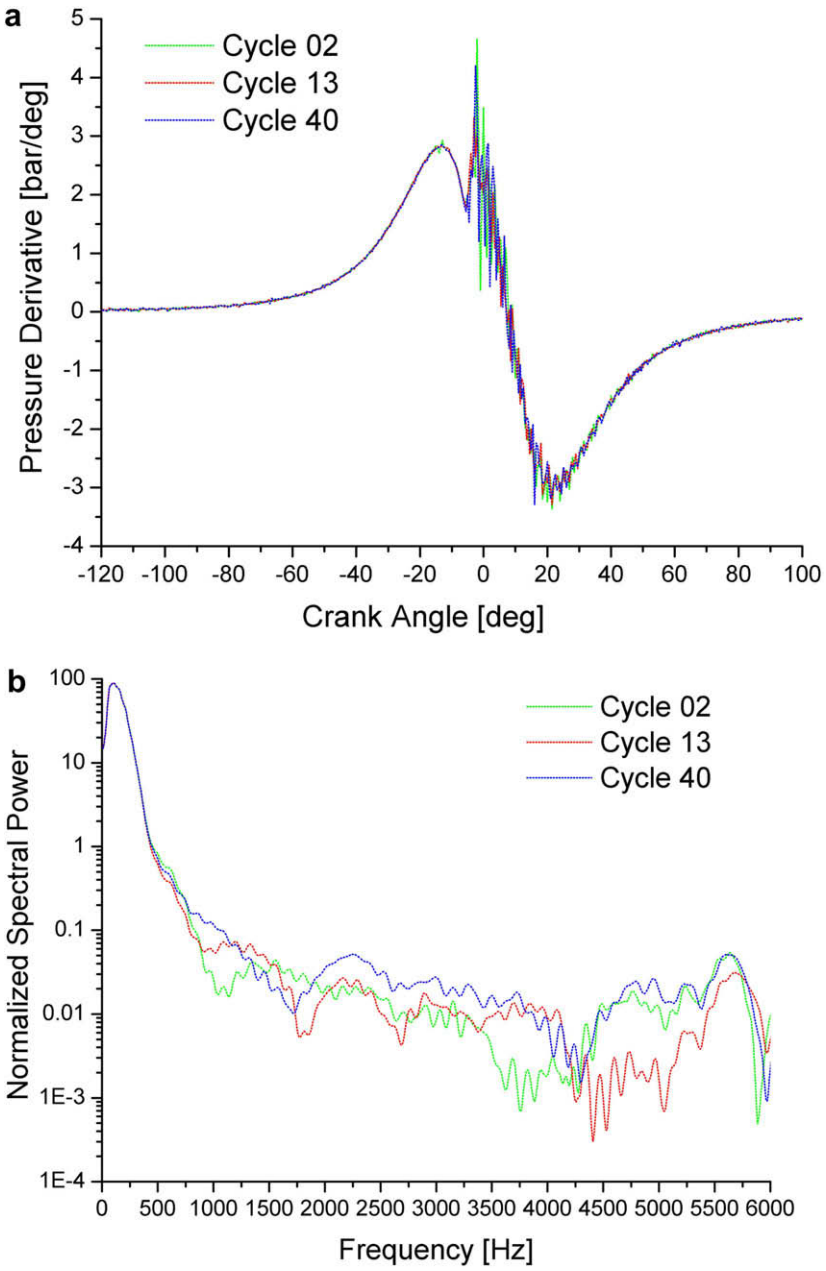

Fig. 10. Pressure derivative experimental data and its spectral composition (2600 rpm and 80% of full load).

The use of the current-to-voltage converter avoids the need of special care with insulation resistances and leakage current, enabling the current polarized by the transducer to flow to ground via a low resistance path. In this case, the non-idealities of the signal conditioning circuit cause an effectively constant offset of the pressure derivative baseline, which can be suppressed with the utilization of an ultra-low bias current operational amplifier. Additionally, the long-term drift also makes the pressure derivative baseline deviate from its original position; however, this effect disappears as the engine operates in steady state. Thus, the circuit shown in Fig. 5 eliminates the need for periodic reset during measurements.

In order to ensure adequate accuracy of experimental data, the measuring chain formed of the piezoelectric transducer, the current-to-voltage converter and the data acquisition system was calibrated using the loading/unloading quasistatic procedure with a deadweight tester, as described by Lancaster et al. [12]. The pressure variation rates experienced by the transducer during this calibration were significantly smaller than those of in-cylinder measurements, a fact that justified applying a gain of 40 dB to the output signal of the current-to-voltage converter. Corresponding pressure data was obtained through numerical integration and this data allowed the determination of an equivalent gain of 5012.52 bar/(s V), as well as a linearity of ±0.322% for the entire measuring system. Fig. 6 shows the obtained pressure curve when the transducer was loaded with 19.61 bar (20 kgf/cm^2) from an initial pressure of 117.68 bar (120 kgf/cm^2).

4. Engine indicating signal and noise characterization

Cylinder pressure data measured by a transducer can be understood as being the sum of two components: (i) a smooth curve, corresponding to the instantaneous average pressure through the entire cylinder volume; and (ii) a spurious component,

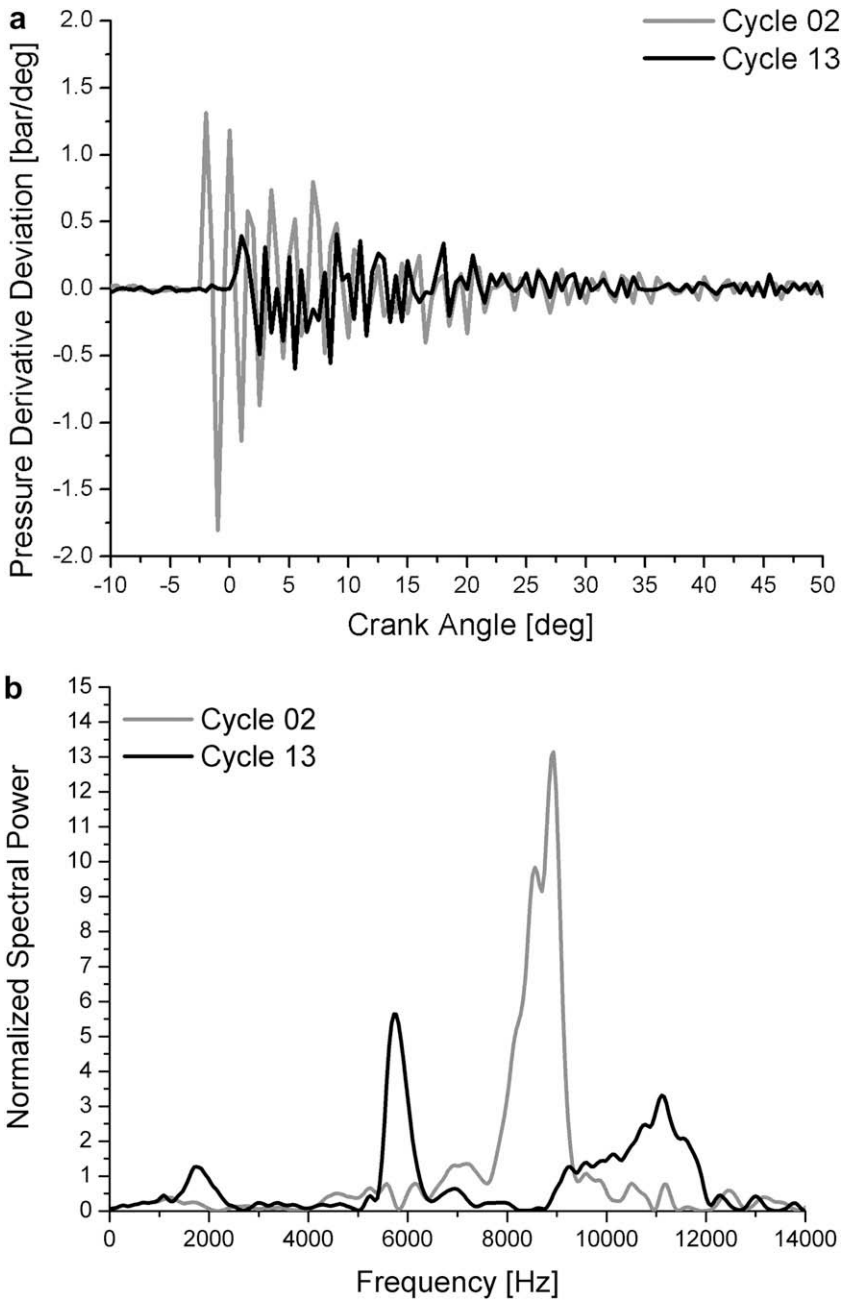

Fig. 11. Combustion driven spurious component in experimental pressure derivative data (2600 rpm and 80% of full load).

originated by both the turbulent flow of gases inside the cylinder and the acoustic pulsations associated to combustion. According to the hypothesis of the single zone combustion model, the first component must be used to characterize the thermodynamic state of the gases in the cylinder, constituting the information of interest for heat release analysis. The second component is small when compared with the first one and its intensity depends on the transducer location in the combustion chamber. In addition to these two components of the measured pressure, the experimental data also include noise generated by the measurement system during the conditioning of the transducer output signal. Thus, for accurate heat release analysis it is necessary to isolate the volume-averaged pressure component from both the flow and the combustion driven spurious components as well as from the measurement noise.

Typically, the isolation of the smooth volume-averaged pressure component has been accomplished by means of numerical treatment of experimental data, which is usually applied after data averaging over several consecutive cycles. A diversity of methods can be used for this numerical treatment, including FFT filters, windowing filters and smoothing splines. However, the choice of a proper data treatment methodology for the engine indicating measurement procedure proposed here requires at least a basic knowledge about the behavior of the above-mentioned components of experimental data. The strategy adopted to assess this behavior consists of estimating at first the smooth curve that corresponds to the average pressure through the entire cylinder volume, which is named the reference curve (Section 4.1) and, then, employing this curve to estimate the spurious components of the experimental data (Sections 4.2 and 4.3).

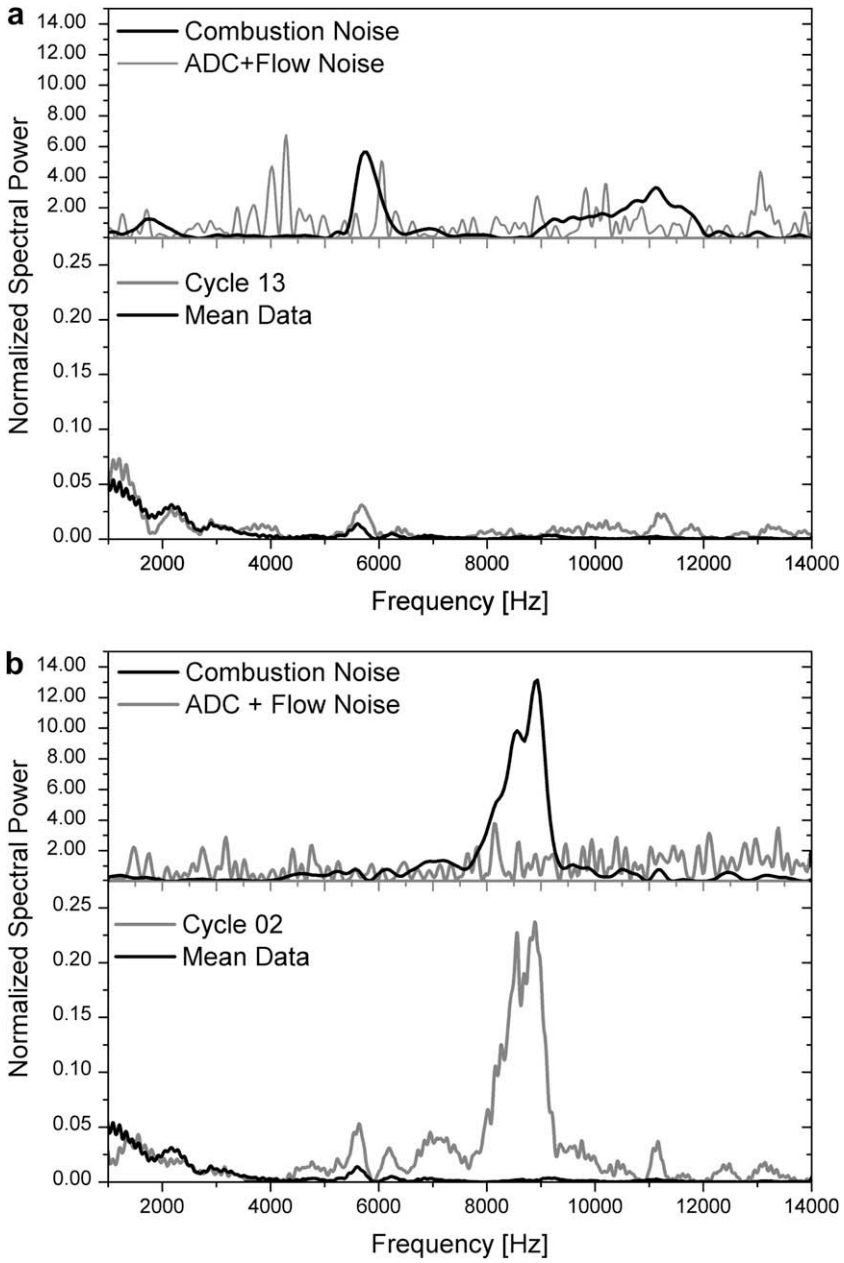

Fig. 12. Noise in individual cycles and its reduction by cycle averaging (2600 rpm and 80% of full load).

4.1. Reference curve for the volume averaged cylinder pressure

Reference curves for both in-cylinder pressure and in-cylinder pressure derivative data were estimated by means of a computer routine that uses a single zone combustion model. In this routine, the heat release rate was represented by two Wiebe functions [24] whose adjusting constants were determined by curve fitting to heat release rate data calculated from experimental data.

Fig. 7 shows reference curves and experimental data obtained with each one of the signal conditioning procedures, for the case of an engine running at 2600 rpm and 80% of full load. The premixed burning causes a steep slope in the pressure curve, subsequent to ignition (circled area in Fig. 7a), whilst in the pressure derivative curve it is reflected as a prominent peak (circled area in Fig. 7b). By comparing these two representations, it becomes evident that the premixed combustion is more visible in the pressure derivative curve, a fact that led to the choice of the pressure derivative as the basic representation for the analysis of the data given by the indicator system.

The frequency domain representations shown in this study employ numerically obtained Lomb periodograms [25]. In these periodograms, the spectral power was normalized with respect to the variance of the analyzed data, and its value represents the degree of participation of the signal associated to a given frequency in the composition of the studied data.

In Fig. 8, spectral distributions of two pressure derivative curves obtained through numerical simulation are compared. The first curve, named *reference data*, was calculated using two Wiebe functions, corresponding to premixed and diffusive stages of combustion, respectively. The second curve, named *diffusive combustion data*, was obtained suppressing the premixed combustion and only one Wiebe function representing diffusive combustion was used.

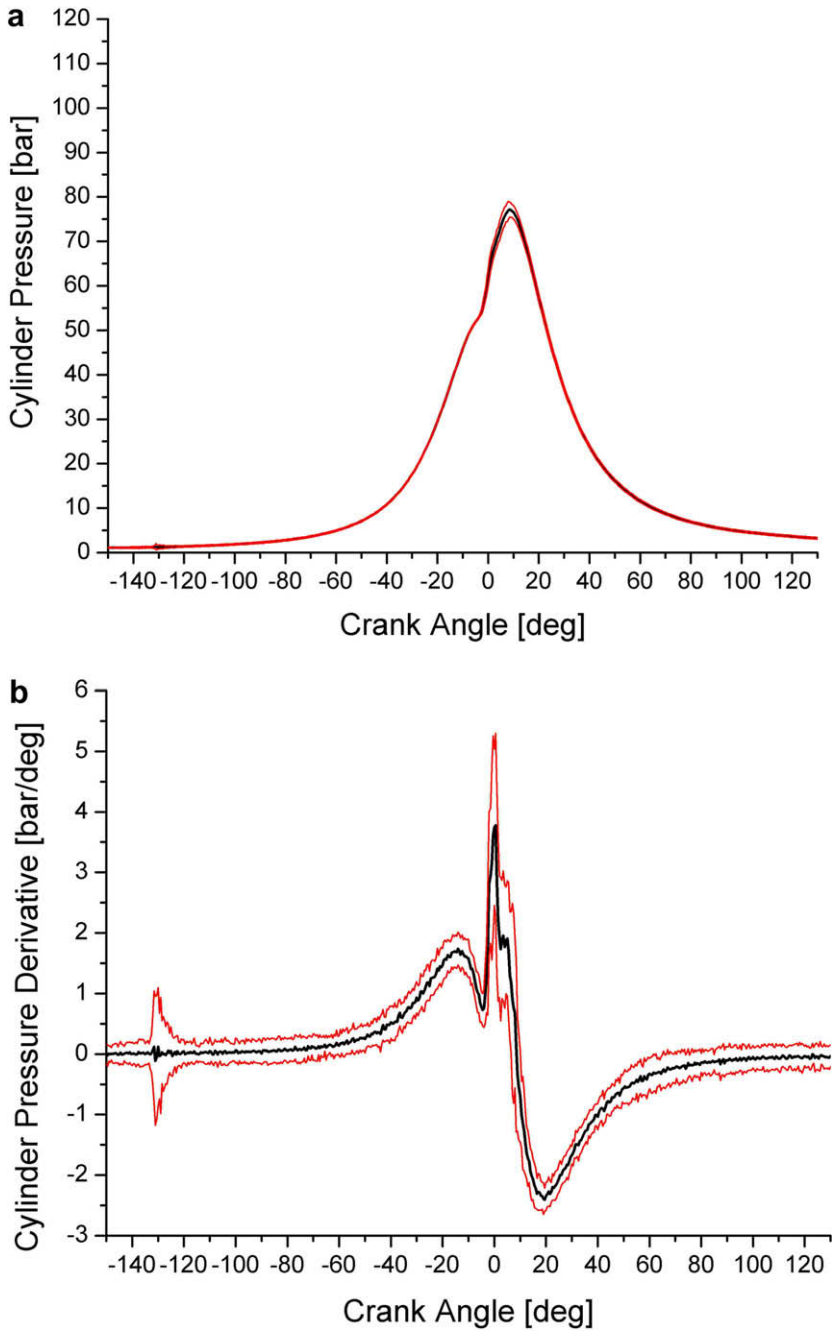

Fig. 13. Indicating data obtained using the charge amplifier: 1400 rpm and 40% load.

As can be seen in Fig. 8, these curves exhibit similar spectral power distribution in the low frequency region (up to 1000 Hz); however, in the region between 1000 and 5000 Hz the suppression of premixed combustion caused considerable attenuation of the pressure derivative data. Thus, it may be concluded that the contribution of the premixed combustion is located in this frequency range (from 1000 to 5000 Hz) and that the utilization of low-pass filters or numerical treatment to smooth the transducer signal at frequencies below 5000 Hz may cause distortion or even the elimination of the influence of premixed combustion on experimental data. It may also be observed that the effects of both the compression process and the diffusive combustion play a major role in the spectral distribution of the data of interest, occupying the frequency range with highest spectral power values (below 1000 Hz).

These considerations are in agreement with the trends reported in the work of Priede [26], where the sound produced during the combustion process in a diesel engine was associated to the in-cylinder pressure rise rate. Priede observed that the low frequency region of the cylinder pressure spectral distribution is similar to that obtained with a motored engine, while in the high frequency region the spectral distribution depends on the pressure rise rate subsequent to ignition, thus being related to the premixed combustion. Payri et al. [27] reported similar results, noting that the low-frequency region of the pressure spectral distribution (under 200 Hz) is clearly dominated by the pseudo-motored signal, while the medium-frequency range (200 Hz-6 kHz) is dominated by the combustion signal.

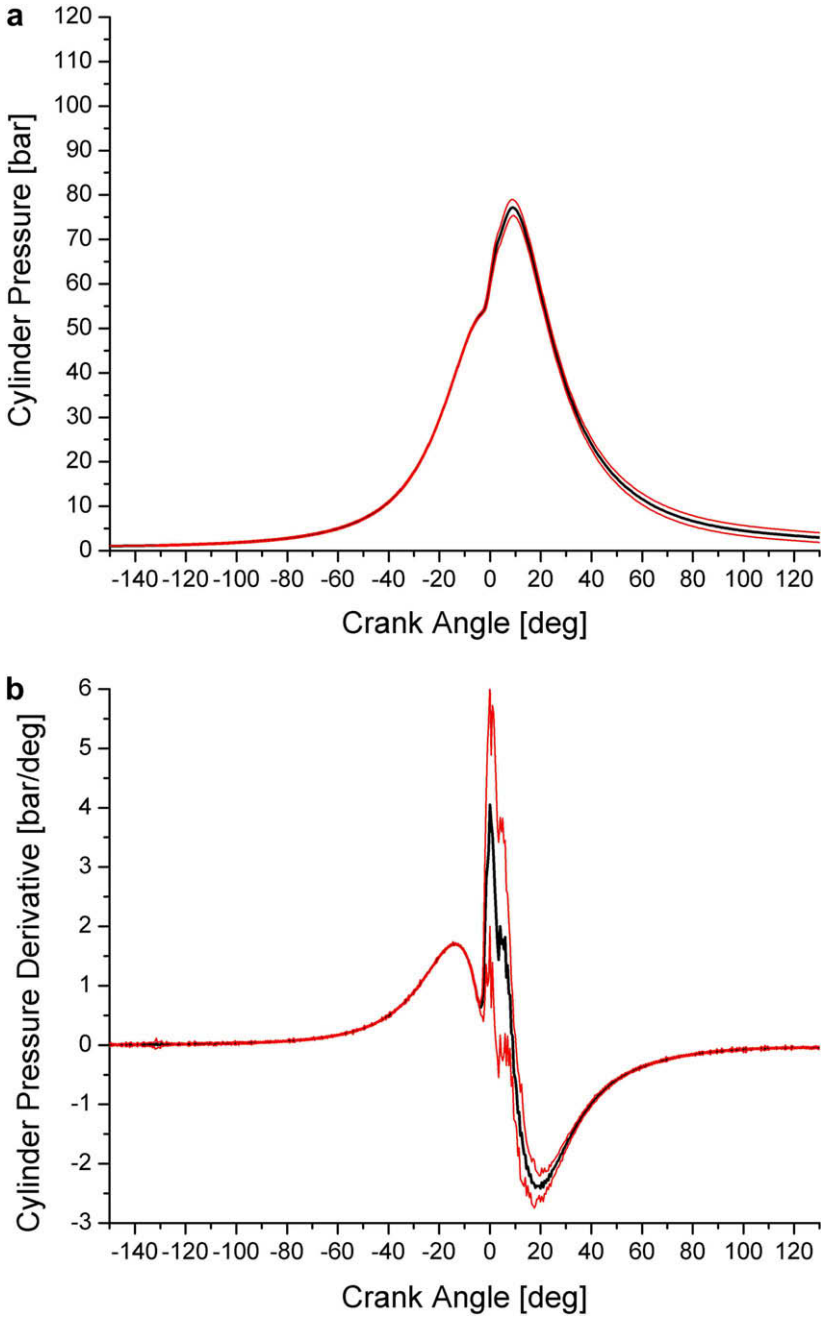

Fig. 14. Indicating data obtained using the current-to-voltage converter: 1400 rpm and 40% load.

4.2. Measurement system noise and the flow driven spurious component

The calculated reference curves were used to estimate the spurious components of the experimental data, which was made by subtracting the experimental data from the corresponding reference curves.

Uncertainties associated to the data acquisition system are dominated by the truncation error of the analog-to-digital converter, acting as a source of white noise in the acquired experimental signal. Therefore, the measurement uncertainty due to this noise (MU) can be estimated in terms of the analog-to-digital converter accuracy, which corresponds to the least-significant bit (LSB) for the measurement system used in this work.

When a transducer is polarized by a charge amplifier, the influence of this uncertainty on the pressure derivative curve is indirect, because the measured parameter in this case is the in-cylinder pressure. Nevertheless, it is possible to estimate the measurement uncertainty imposed by the quantization noise to the pressure derivative (MU_{dP}) using Eq. (3) and taking into account that for this measurement the LSB value was 0.131 bar:

$$MU_{dP} = \pm\sqrt{\left(\left(\frac{LSB}{12\Delta\theta}\right)^2 + \left(\frac{-8LSB}{12\Delta\theta}\right)^2 + \left(\frac{8LSB}{12\Delta\theta}\right)^2 + \left(\frac{-LSB}{12\Delta\theta}\right)^2\right)} = \pm 0.25\ \text{bar}/^\circ \quad (5)$$

On the other hand, when the direct polarization of the transducer is used, the pressure derivative is accessed directly and the mea-

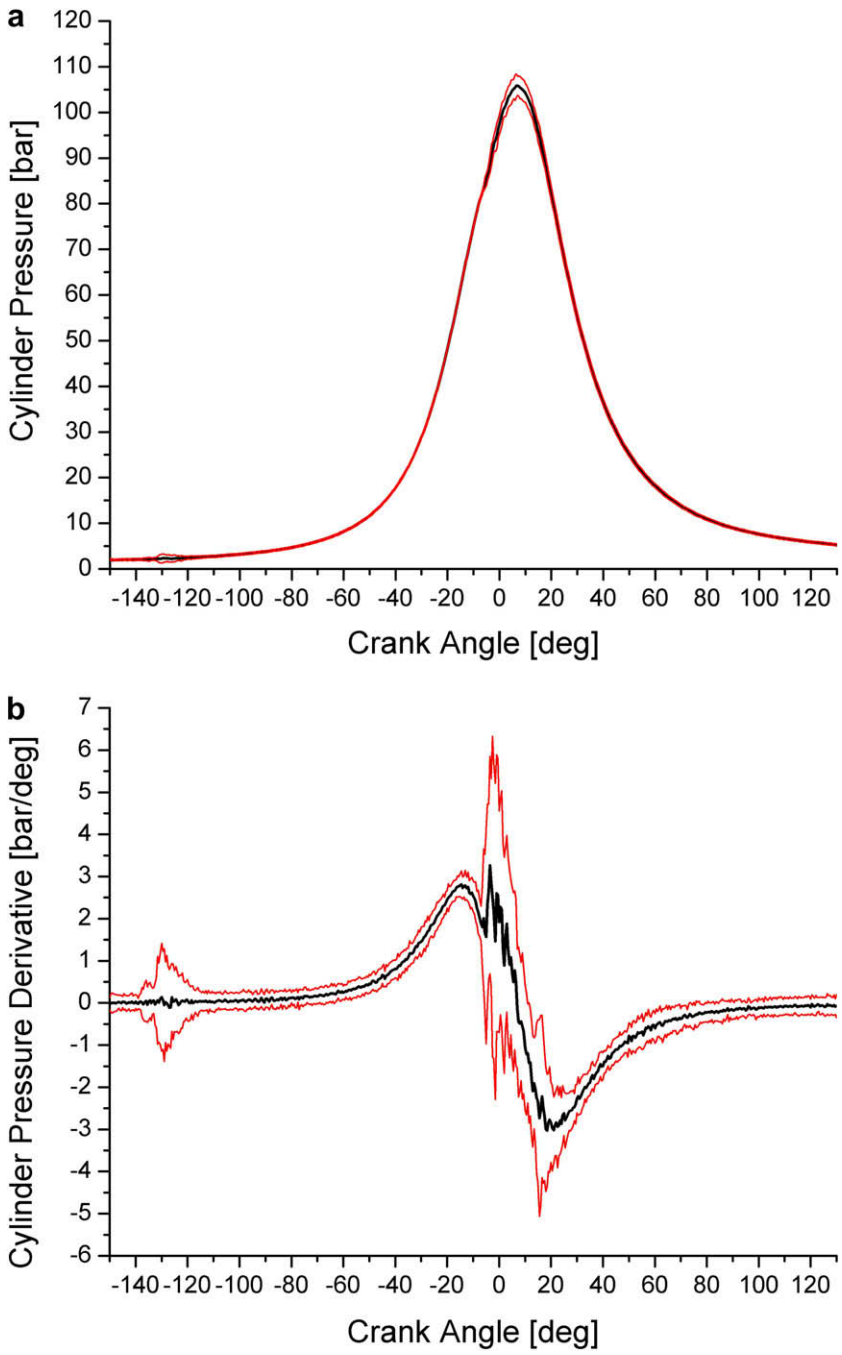

Fig. 15. Indicating data obtained using the charge amplifier: 2600 rpm and 80% load.

surement uncertainty imposed by the quantization noise to the pressure derivative is given by the corresponding LSB value (54.694 bar/s):

$$MU_{dP} = \pm 54.694 \text{ bar/s} = \pm 3.5 \times 10^{-3} \text{ bar/}^{\circ} \quad (6)$$

It must be noticed that the utilization of a current-to-voltage converter allows the measurement uncertainty imposed by the quantization noise to be reduced to only 1.4% of the corresponding value obtained using a charge amplifier. As it will be discussed later, this fact has important consequences for obtaining smooth heat release rate diagrams. Additionally, when signal conditioning is carried out using a charge amplifier, the refinement of the encoder resolution increases the measurement uncertainty, whilst for the case of the proposed procedure the measurement uncertainty does not depend on the encoder resolution.

Fig. 9a exhibits deviation curves of the experimental data respective to the reference pressure derivative curve during the compression process, when combustion does not occur and, therefore, the spurious components of the experimental data can be attributed only to the in-cylinder flow and to the data acquisition system. It may be observed in this figure that the utilization of a charge amplifier imposes oscillations, which are within the limits of the quantization noise (±0.25 bar/°); whilst for the case of the current-to-voltage converter these oscillations exceed the corresponding limits ($\pm 3.5 \times 10^{-3}$ bar/°). Therefore, it is possible to conclude that the utilization of a charge amplifier makes the effects of the noise generated by

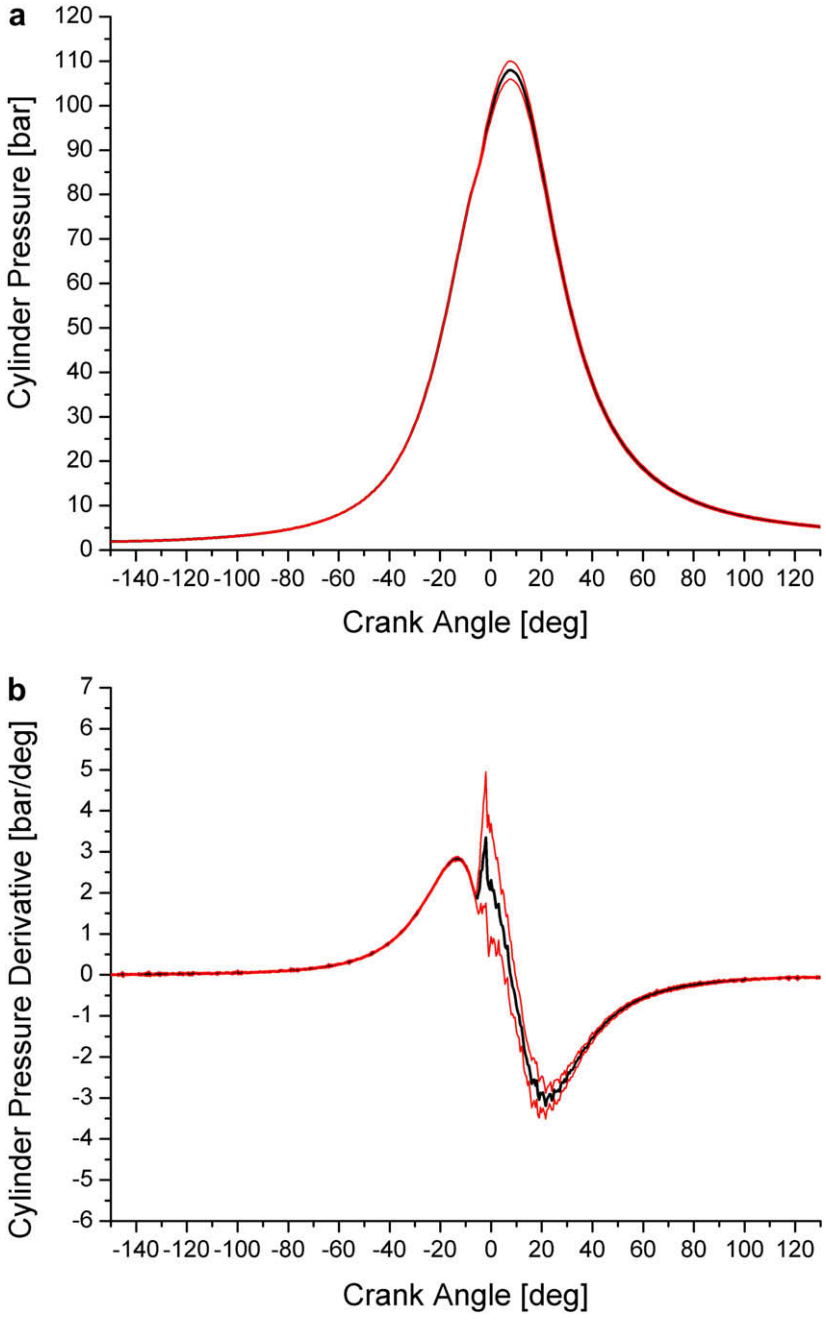

Fig. 16. Indicating data obtained using the current-to-voltage converter: 2600 rpm and 80% load.

the data acquisition system be predominant over the spurious component generated by in-cylinder flow, whilst in the case of the proposed procedure the oscillations registered during the compression process are mainly driven by the in-cylinder flow.

The spectral distributions corresponding to the deviation curves shown in Fig. 9a can be found in Fig. 9b. These distributions characterize both the in-cylinder flow as well as the quantization error, as sources of white noise (random noise), having a considerable part of its spectral composition in the same frequency range occupied by the data of interest. Such behavior makes it difficult to use low-pass filters or numerical smoothing without loss of useful signal, demanding especial care during the choice of the smoothing parameters, which vary with engine running condition [28].

Due to the strong presence of the quantization noise in the data obtained with the charge amplifier, the remaining analysis of the experimental data composition was based on the proposed experimental approach.

4.3. The combustion driven spurious component

The ignition in diesel engines exhibits an eminently chaotic character, being strongly influenced by the interaction of chemical and hydrodynamic phenomena occurring along the ignition delay [29]. Because of this, a diesel engine operating in steady state presents cycle-to-cycle variations in the amount of fuel available for the premixed combustion as well as in the location where the ignition occurs. In addition, the natural vibration modes of the gas contained in the cylinder are excited by the high

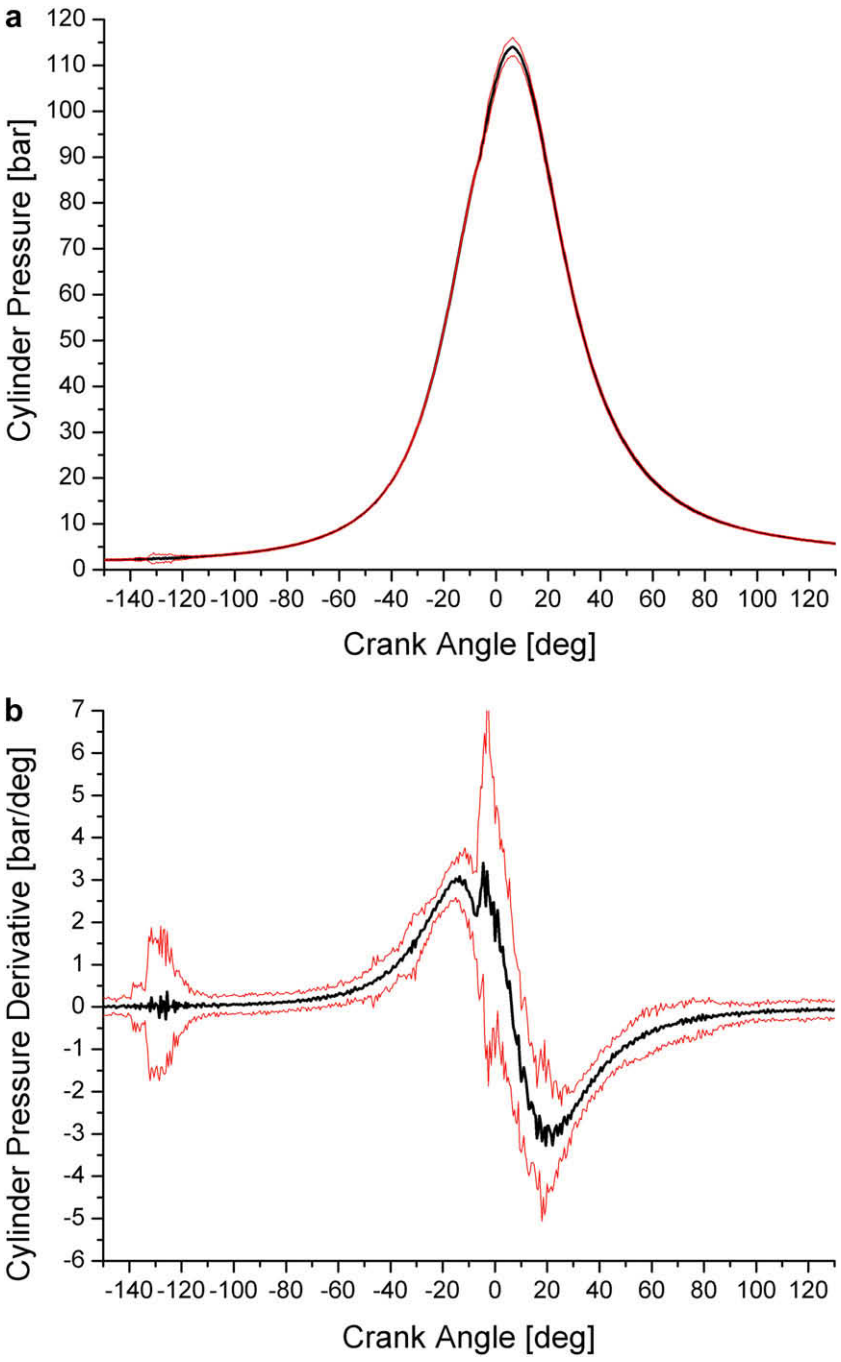

Fig. 17. Indicating data obtained using the charge amplifier: 2900 rpm and full load.

burning rates that occur in the beginning of the combustion [26,30], generating pressure oscillations of large amplitude that are rapidly dampened due to the high area/volume ratio of the cylinder cavity [30]. Due to cycle-to-cycle combustion variability, different modes are excited in each cycle, causing the oscillations to vary in phase, characteristic frequencies and amplitude from one cycle to another.

Fig. 10a shows the typical behavior of experimental pressure derivative data, where the cycle-to-cycle variability associated to the premixed combustion and to the following acoustic oscillations contrasts with the repeatability inherent to both the compression process and the diffusive combustion. In the periodograms presented in Fig. 10b, the combustion-generated variability appears in the frequencies above 1000 Hz. This result is in accordance with the observations of Stahle et al. [31–33], who attributed the pressure data spectrum above 1000 Hz to the random nature phenomena associated to the combustion.

In Fig. 11a the deviations of the experimental data respective to the reference pressure derivative curve are shown for two different cycles during combustion. As can be noticed, after 25° c.a. the amplitude of the oscillations is dampened to a constant level slightly higher than that observed during compression, indicating that the combustion process amplifies the influence of the flow turbulence on the experimental data. The spectral analysis of this deviation is shown in Fig. 11b, where the presence of a periodic sig-

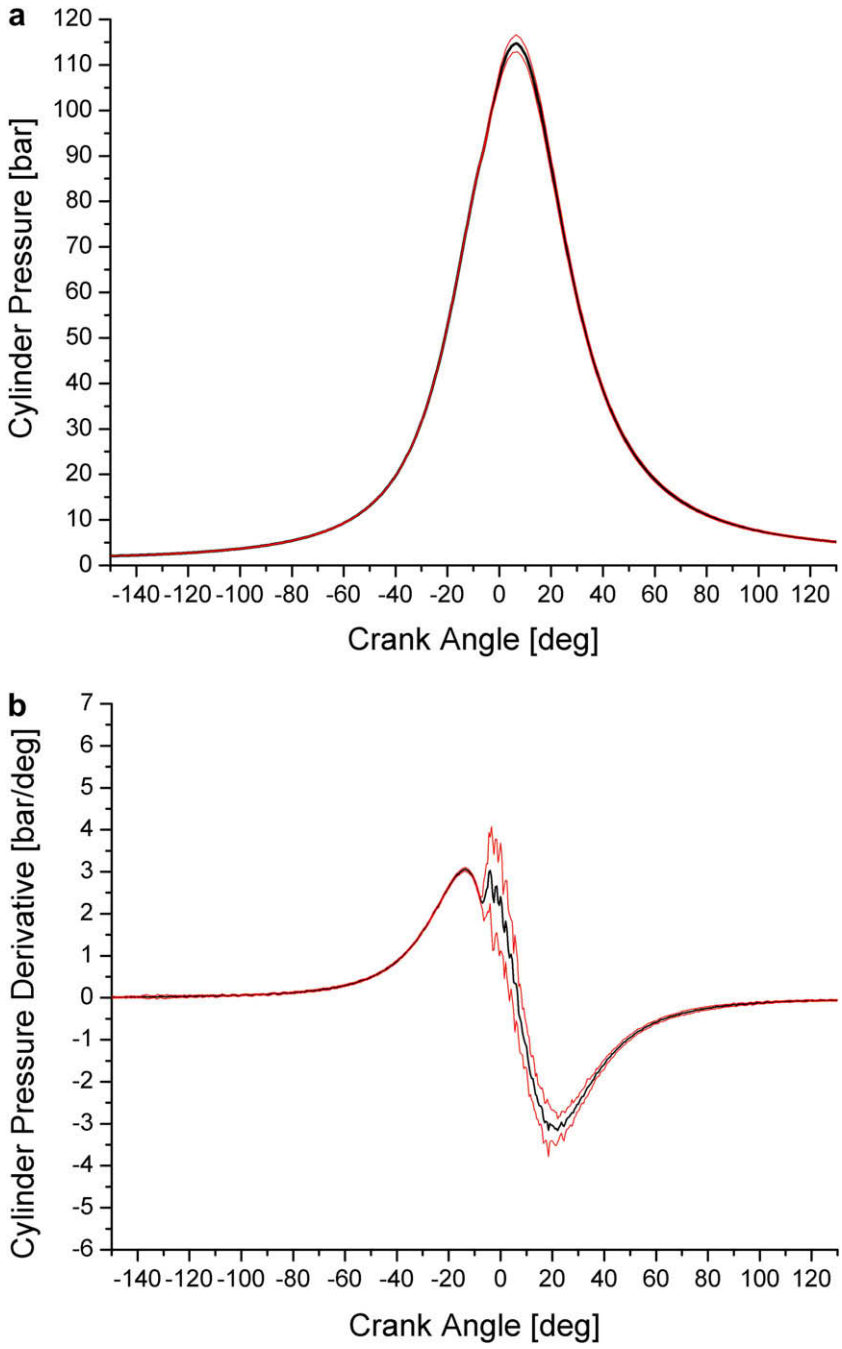

Fig. 18. Indicating data obtained using the current-to-voltage converter: 2900 rpm and full load.

nal in frequencies that should correspond to characteristic frequencies of the cylinder cavity can be seen (9 kHz for cycle 2; and 2, 6 and 11 kHz for cycle 13). Fig. 11a and b confirm that the oscillations vary in phase, in characteristic frequencies and in amplitude from one cycle to other. This behavior is used in Section 5 to remove the combustion driven oscillations by data overlapping.

5. Experimental data treatment

Due to the behavior of the spurious components of the experimental data, cycle-averaging carried out over a significant number of successive cycles became an effective method of data treatment, easing the effects of cycle-to-cycle variations, combustion driven oscillations and measurement noise by data overlapping. This can be seen in Fig. 12, which shows in its upper part the spectral composition of the spurious components of experimental data, whilst in its lower part the spectral composition of single-cycle pressure derivative data is compared to that of mean data (averaged over a sequence of 56 cycles). Data corresponding to cycles with the lowest noise level (13th cycle) and with the highest noise level (second cycle) are shown in the left and in the right parts of this figure, respectively.

6. Results and discussion

Figs. 13–18 show diagrams of cylinder pressure and its derivative obtained from the two studied transducer signal conditioning

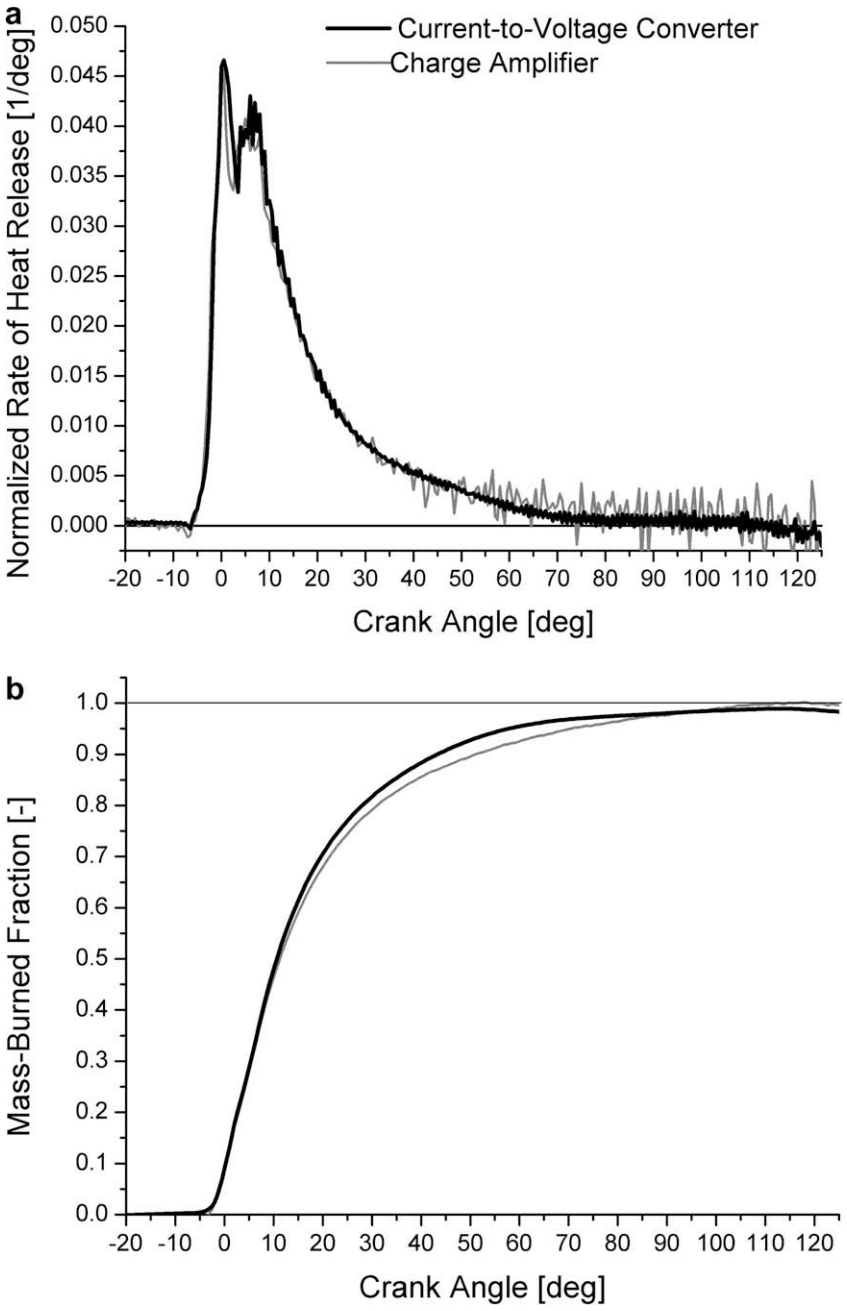

Fig. 19. Normalized heat release rate and fuel mass burned fraction: 1400 rpm and 40% load.

procedures. Curves obtained by cycle averaging over 56 consecutive cycles are shown together with their 95% confidence limits. The data reported in these figures correspond to three engine operating conditions: 1400 rpm and 40% load; 2600 rpm and 80% load; and 2900 rpm and full load.

Both transducer signal conditioning procedures resulted in similar values for the cycle averaged cylinder pressure and its confidence limits (Figs. 13–18a), so that it may be concluded that both approaches are equivalent when the cylinder pressure is the data of interest. However, the studied procedures gave different results when evaluating pressure derivative, which is the data of greater interest for heat release analysis. As can be noticed in Figs. 13–18b, the pressure derivative confidence interval obtained with the current-to-voltage converter was smaller than that obtained using the charge amplifier and subsequent numerical derivation, the former reaching only about 1/50 of the latter during most of the compression process as well as during late combustion, as predicted in Section 4.2. Yet throughout the main combustion as well as soon after the closing of the admission valves, when noise is generated by the diesel combustion and by the admission flow, respectively, the confidence interval obtained with the current-to-voltage converter was constantly reduced as the engine speed and load increased.

Considering the extension of the confidence intervals of pressure derivative data, it is expected that heat release results calculated from the charge amplifier data exhibit a more irregular and oscillatory pattern than those calculated from the current-to-voltage converter data. It is worth mentioning that large oscillations in the calculated heat release rate can result in negative values during the compression as well as during late combustion, which makes

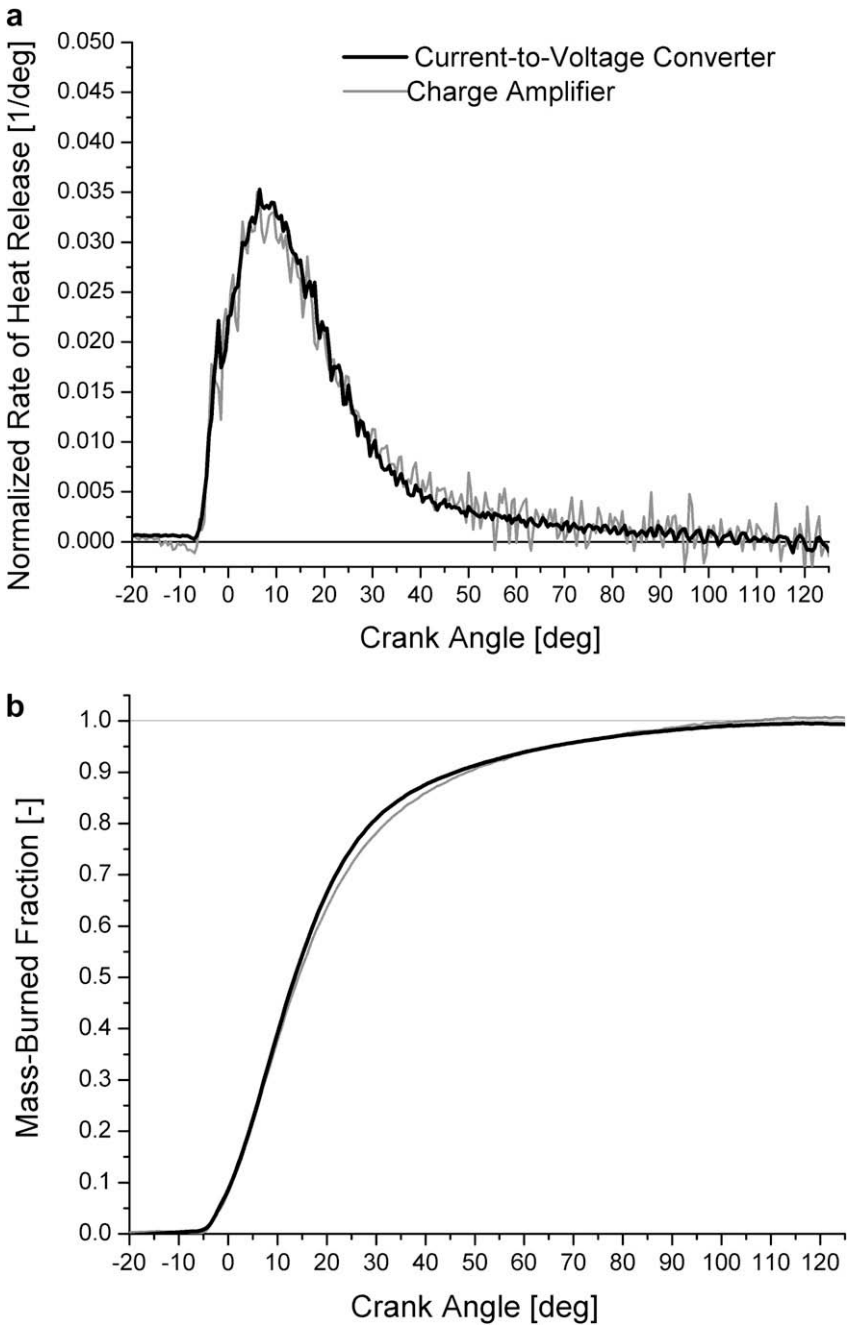

Fig. 20. Normalized heat release rate and fuel mass burned fraction: 2600 rpm and 80% load.

no physical sense. These oscillations make it difficult to determine the pressure data baseline, which in turn increases the uncertainty in the assessment of the burned fraction of fuel mass. The data shown in Figs. aa19–21a confirms that heat release curves calculated from charge amplifier data exhibit a higher noise level than those calculated from current-to-voltage converter data, while Figs. 19b, 20b and 21b give evidence of the differences in the calculated burned fraction of fuel mass, which are caused by this higher noise level.

7. Conclusions

A novel engine indicating measurement procedure for heat release analysis has been presented. This procedure is based on the direct measurement of the current supplied by the transducer, avoiding the use of complex polarization circuits such as those based on the use of charge amplifiers. The proposed procedure permits the direct measurement of the pressure derivative, which is the main data for calculating combustion heat release rate.

The analysis conducted in this work allowed the estimation of the experimental data smooth component, which is related to the instantaneous average pressure through the cylinder volume, as well as its isolation from the flow and from the combustion driven spurious components, and from the quantization noise.

It was verified that the conversion of the current supplied by a piezoelectric transducer into an analog signal reduces the quantization noise of pressure derivative data by about 70 times. Furthermore, the association of this signal conditioning procedure with

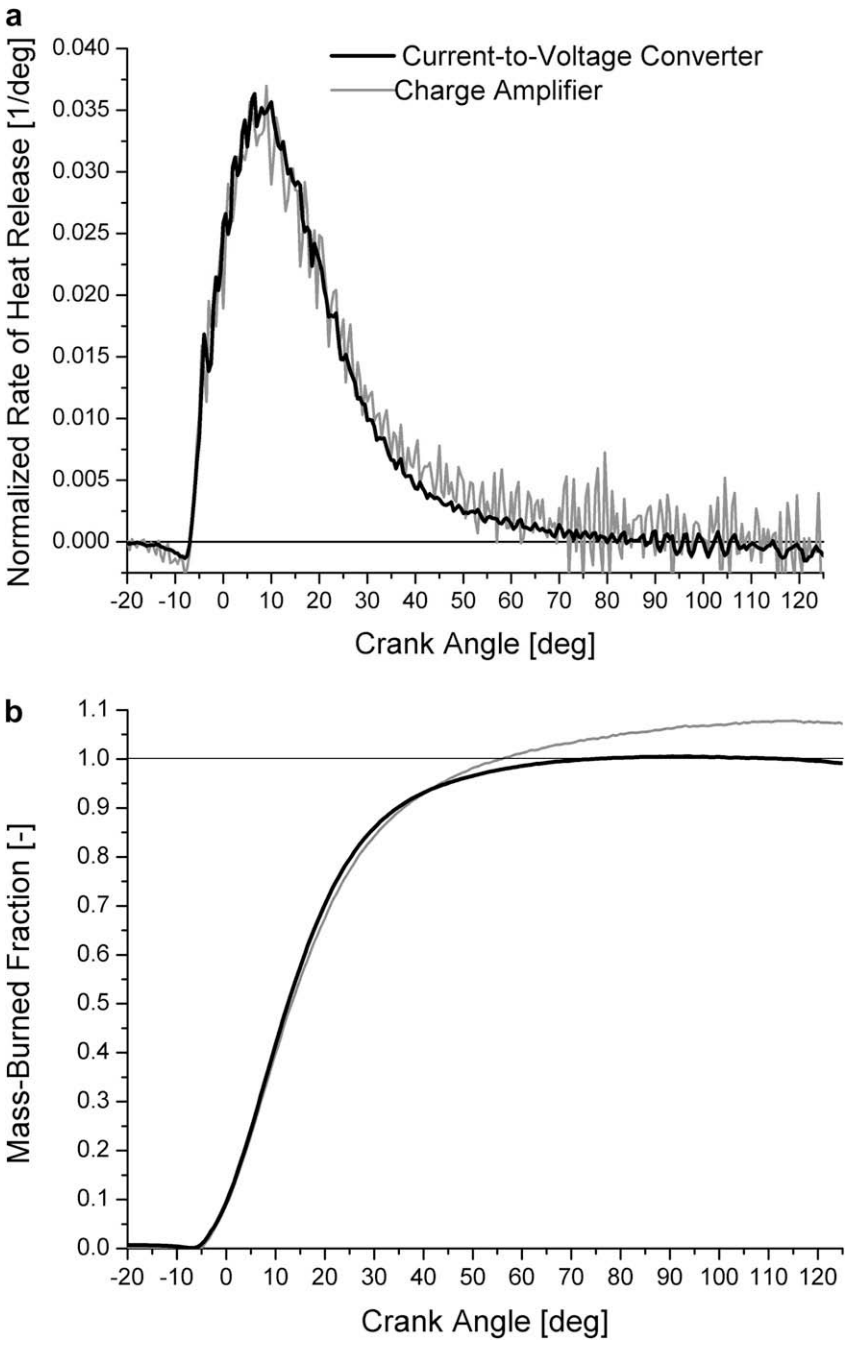

Fig. 21. Normalized heat release rate and fuel mass burned fraction: 2900 rpm and full load.

cycle averaging as data treatment methodology allowed obtaining curves of heat release rate with reduced spurious oscillations.

References

[1] G.M. Rassweiler, L. Withrow, Motion pictures of engine flames correlated with pressure cards, SAE Transactions 38 (1938) 185–204.
[2] G. Woschni, Computer programs to determine the relationship between pressure, flow, heat release and thermal load in diesel engines, SAE Paper, 1965, 650450.
[3] R.B. Krieger, G.L. Borman, The computation of apparent heat release for internal combustion engines, ASME paper 66-WA/DGP-4, 1966.
[4] J.A. Gatowski, E.N. Balles, K.N. Chun, F.E. Nelson, J.A. Ekchian, J.B. Heywood, Heat release analysis of engine pressure data, SAE Paper, 1984, 841359.
[5] W.T. Lyn, Diesel combustion study in infrared emission spectroscopy, Journal of the Institute of Petroleum 43 (1957) 25.
[6] W.T. Lyn, E. Valdmanis, The application of high speed schlieren photography to diesel combustion research, Journal of Photo Science 10 (1962) 74–82.
[7] A.E.W. Austen, W.T. Lyn, Relation between fuel injection and heat release in a direct-injection engine and the nature of the combustion processes, Proceedings of the Institution Mechanical Engineers 1 (1960–1961) 47–62.
[8] W.T. Lyn, Study of burning rate and nature of combustion in diesel engines, Proceedings of the Combustion Institute 9 (1962) 1069–1082.
[9] J.B. Heywood, Internal Combustion Engine Fundamentals, McGraw-Hill, New York, USA, 1988.
[10] J.E. Dec, A conceptual model of DI diesel combustion based on laser-sheet imaging, SAE Paper, 1997, 970803.
[11] D.J. Timoney, Problems with heat release analysis in D.I. diesels, SAE Paper, 1987, 870270.
[12] D.R. Lancaster, R.B. Krieger, J.H. Lienesch, Measurement and analysis of engine pressure data, SAE Paper, 1975, 750026.
[13] M. Lapuerta, O. Armas, V. Bermúdez, Sensitivity of diesel engine thermodynamic cycle calculation to measurement errors and estimated parameters, Applied Thermal Engineering 20 (2000) 843–861.
[14] S. Lee, C. Bae, R. Prucka, G. Fernandes, Z. Filipi, D. Assanis, Quantification of thermal shock in a piezoelectric pressure transducer, SAE Paper, 2005, 2005-01-2092.

[15] R. Pischinger, J. Glaser, Problems of pressure indication in internal combustion engines, in: Proceedings of COMODIA 1985, Tokyo, Japan, 1985.
[16] W.L. Brown, Methods for evaluating requirements and errors in cylinder pressure measurement, SAE Paper, 1967, 670008.
[17] R.S. Benson, R. Pick, Recent advances in internal combustion engine instrumentation with particular reference to high-speed data acquisition and automated test bed, SAE Paper, 1974, 740695.
[18] M. Marzouk, N. Watson, Some problems in diesel engine research with special reference to computer control and data acquisition, Proceedings of the Institution Mechanical Engineers 190 (1976) 137–151.
[19] A.L. Randolph, Methods of processing cylinder-pressure transducer signals to maximize data accuracy, SAE Paper, 1990, 900170.
[20] K.J. Roth, A. Sobiesiak, L. Robertson, S. Yates, In-cylinder pressure measurements with optical fiber and piezoelectric transducers, SAE Paper, 2001, 2002-01-0745.
[21] R.S. Benson, N.D. Whitehouse, Internal Combustion Engines, first ed., Pergamon Press, 1983.
[22] K.W. Morton, D.F. Mayers, Numerical Solution of Partial Differential Equations, Cambridge University Press, 1994.
[23] F. Payri, S. Molina, J. Martín, O. Armas, Influence of measurement errors and estimated parameters on combustion diagnosis, Applied Thermal Engineering 26 (2006) 226–236.
[24] J.J. Wiebe, Brennverlauf und Kreisprozes von Verbrennungsmotoren, VEB-Verlag Technik Berlin, Germany, 1970.
[25] N.R. Lomb, Least-squares frequency analysis of unequally spaced data, Astrophysics and Space Science 39 (1976) 447–462.
[26] T. Priede, Relation between form of cylinder pressure diagram and noise in diesel engines, Proceedings of the Institution Mechanical Engineers 1 (1961) 63–77.
[27] F. Payri, A. Broatch, B. Tormos, V. Marant, New methodology for in-cylinder pressure analysis in direct injection diesel engines – application to combustion noise, Measurement Science and Technology 16 (2005) 540–547.
[28] L. Zhong, N.A. Henein, W. Bryzik, Effect of smoothing the pressure trace on the interpretation of experimental data for combustion in diesel engines, SAE Paper, 2004, 2004-01-0931.
[29] B. Maunoury, T. Duverger, K. Mokaddem, F. Lacas, Phenomenological analysis of injection, auto-ignition an combustion in a small D.I. diesel engine, SAE Paper, 2002, 2002-01-1161.
[30] K. Schmillen, M. Schneider, Combustion chamber pressure oscillations as a source of diesel engine noise, in: Proceedings of COMODIA 1985, Tokyo, Japan, 1985.
[31] W.C. Strahle, J.C. Handley, M.S. Varma, Cetane rating and load effects on combustion noise in diesel engines, Combustion Science and Technology 17 (1977) 51–61.
[32] W.C. Strahle, Combustion randomness and diesel engine noise: theory and initial experiments, Combustion and Flame 28 (1977) 279–290.
[33] W.C. Strahle, M. Muthukrishnan, J.C. Handley, Turbulent combustion and diesel engine noise, Proceedings of the Combustion Institute 16 (1977) 337–346.